

Nuclear interactions of defects in semiconductors – magnetic resonance measurements

C.A.J. Ammerlaan, S.J.C.H.M. van Gisbergen, N.T. Son and T. Gregorkiewicz

Van der Waals – Zeeman Laboratorium, Universiteit van Amsterdam, Valckenierstraat 65, NL-1018 XE Amsterdam, Netherlands

Nuclear interactions, such as the Zeeman, hyperfine and quadrupole energies, of paramagnetic centres in semiconductors were studied by magnetic resonance. Both electron paramagnetic resonance (EPR) and electron–nuclear double resonance (ENDOR) were profitably applied. The implementation of these methods in order to obtain the relevant data is described, along with their use in the devising of defect structure models. Examples illustrating the discussion include the centres GaP:Mn_i²⁺, Si:ZnCr, Si:S₂⁺, Si:Ni_s⁻, Si:Ti_i⁺ and Si:TD⁺.

1. Introduction

Magnetic resonance measurements form a family of spectroscopic measurements in which the energy level structure related to the spins of electrons and nuclei is probed. The basic forms are nuclear magnetic resonance [1,2] – NMR – and electron paramagnetic resonance [3] – EPR. In the common implementation of these experiments a magnetic field is applied to the system under investigation and transitions between the levels are induced by an electromagnetic field. Magnetic fields are typically about 1 T; the required stimulating fields are then in the radiofrequency range of several MHz for NMR and in the microwave range of several GHz for EPR. Energy level positions are conveniently described using the powerful concept of the spin Hamiltonian, in which energies are expressed as a function of the external fields and the system parameters. The latter involve basically the (effective) electron spin S and the nuclear spin(s) I . The spin Hamiltonian gives the energies using a small number of coupling constants, which in general have a tensor form. In expressing the form of the tensors the crystallographic symmetry of the centre is, to great advantage, taken into account. Transitions in these resonances are broadened by several processes which can be of homo-

geneous or inhomogeneous nature. A best resolution can typically be of order 10^{-4} , which means on the order of kHz for NMR and MHz for EPR. Obviously NMR is superior in this respect. Unfortunately, due to the small quanta involved, the sensitivity of NMR is relatively poor. Its application requires the presence of high concentrations (about 10^{-3}) of magnetic impurities. This usually does not correspond to the conditions under which one wishes to study the doped semiconductor. This serious handicap is the reason why straight NMR is not often applied in semiconductor research. EPR involves the more energetic microwave quanta and extends down to concentrations of about 10^{-9} . It is consequently widely applied for defect and impurity studies. Nuclear interactions are not directly revealed by EPR as only the electron spin quantization is affected, while the nuclei have a passive role. The purely nuclear information therefore remains hidden unless it can be derived on a more exotic basis. Both forms of spectroscopy thus have their specific attractions but also their limitations. The combination of the two forms of spectroscopy in a double resonance experiment can to a great extent combine the advantages, while avoiding the weaknesses. In the method of electron–nuclear double resonance [4] – ENDOR – this idea is implemented. At the cost of extra complexity in

Table 1
Features of the magnetic resonance techniques

	Information		Sensitivity	Resolution	Complexity
	Nuclear	Electronic			
NMR	yes	no	poor	kHz	standard
EPR	no	yes	good	MHz	standard
ENDOR	yes	yes	good	kHz	laborious

building and operation of equipment, this powerful form of spectroscopy can be used to obtain intrinsically coherent information on the electronic and nuclear spins in the centre. The features of the magnetic resonance techniques are summarized in table 1.

This paper gives a brief summary of the application of magnetic resonance in which information of the nuclear structure is obtained. As the paper is brief the reference to the original extensive literature and the books and papers on the basics is an essential supplementary source of information. In the next section examples are given of the extraction of information on nuclear parameters from the EPR and ENDOR spectra. The interpretation of these data in terms of physical models for the atomic and electronic structure of centres is then dealt with, also on the basis of a few examples, in the final section.

2. Magnetic resonance measurements

2.1. Electron paramagnetic resonance

2.1.1. Forbidden transitions

Strongest transitions are induced by the microwave field, frequency ω , acting on the spins via the interaction term $g_e \mu_B \mathbf{S} \cdot \mathbf{B} \cos \omega t$. These transitions obey the rules $\Delta m_S = \pm 1$ and $\Delta m_I = 0$. As the nuclear quantum number m_I does not change, the nuclear energies do not appear in the transition energy. This would be different if the standard quantization of levels in terms of m_S and m_I by the Zeeman energies were perturbed by the presence of other strong interactions. Then, due to mixing of states of different quantum number m_I , transitions which are normally forbidden can appear with comparable or even predominant intensity. In such transitions, with $\Delta m_I \neq 0$, the nuclear energies occur to first order and are thus directly measurable.

An illustration of the practical exploitation of forbidden line structure is provided by the EPR spectrum reported recently for interstitial manganese in gallium phosphide [5]. The spectrum as measured at X- and K-band frequencies is given in fig. 1. For its analysis the spin Hamiltonian

$$H = +g_e \mu_B \mathbf{B} \cdot \mathbf{S} + A \mathbf{S} \cdot \mathbf{I} - g_N \mu_N \mathbf{B} \cdot \mathbf{I} \quad (1)$$

is used. As the spectrum is isotropic, the centre has a cubic symmetry and the constants in the spin Hamiltonian are scalar numbers. The central position gives $g_e = 2.0011$. The six components of equal intensity and (almost) equal separation immediately indicate the presence of a single nucleus with nuclear spin $I = 5/2$ and abundance of 100%. From the separation between main lines it follows that $A/h = 266$ MHz. Due to perturbing terms, not included in the spin Hamiltonian

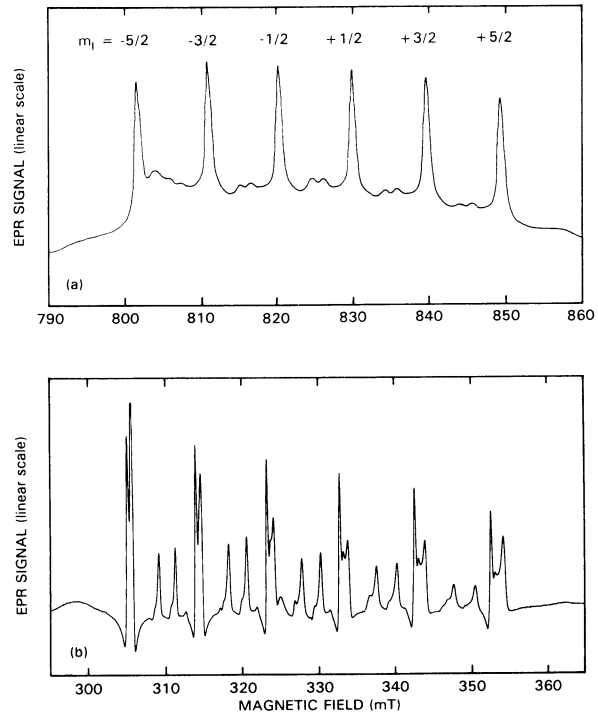


Fig. 1. (a) EPR spectrum of the centre GaP:Mn measured at microwave frequency in the K-band. The allowed transitions are labelled with their m_I quantum number. (b) EPR spectrum of the same centre measured in the microwave X-band.

of eq. (1), states will be mixed. Forbidden transitions are observed in pairs between the main lines and, as expected, they are stronger at the lower X-band energies. According to the Hamiltonian the splitting of lines in the pairs is given by [6–8]

$$\Delta B = 2g_N \mu_N B / g_e \mu_B + \left(S^2 + S - \frac{1}{4}\right) A^2 / g_e^2 \mu_B^2 B - \left(2S^2 + 2S - \frac{3}{4}\right) (2m_I - 1) A^3 / g_e^3 \mu_B^3 B^2. \quad (2)$$

On the basis of this equation the nuclear Zeeman interaction is found to be $g_N \mu_N / h = (10.5 \pm 0.5)$ MHz/T. This result identifies the impurity as Al or Mn. In addition the electron spin is fixed at $S = 5/2$.

An example where only forbidden lines are observed is given by the EPR of the ZnCr impurity pair in silicon [9]. The true electron spin of the centre is $S = 3/2$, but as a result of a strong trigonal crystal field the spin quartet is split into two isolated doublets. The spectrum as given in fig. 2 was observed in a sample with zinc doping enriched in the isotope ^{67}Zn , which has $I = 5/2$. The normal splitting by hyperfine interaction into six components is completely suppressed. Instead five lines related to forbidden transitions with $\Delta m_I \neq 0$ form the spectrum. Analysis is based on a spin Hamiltonian as in eq. (1), but with the zero-field split-

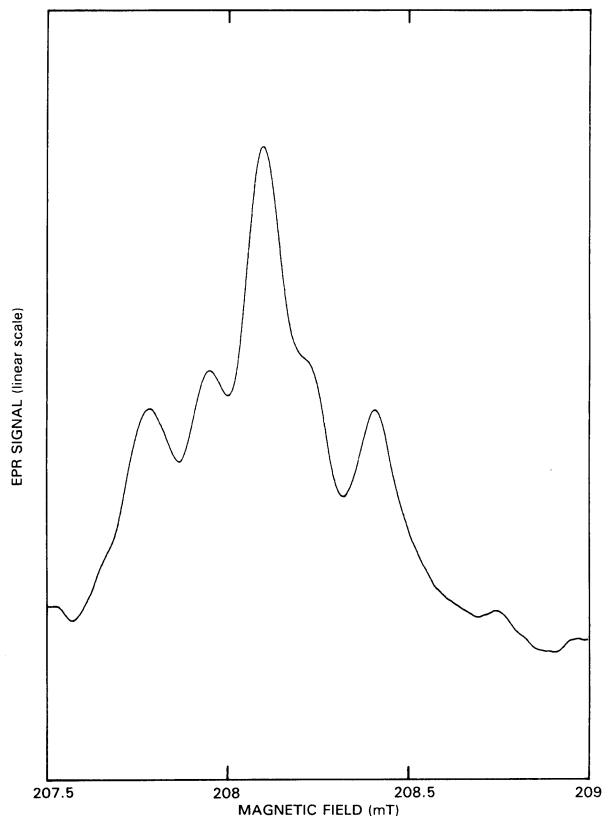


Fig. 2. EPR spectrum of the Si:ZnCr centre, zinc doped sample enriched to 91.9% in the isotope ^{67}Zn with nuclear spin $I = 5/2$, microwave frequency $\nu \approx 9$ GHz.

ting term $S \cdot D \cdot S$ and quadrupole interaction $I \cdot Q \cdot I$ added. The appropriate spin Hamiltonian is

$$H = +\mu_B \mathbf{B} \cdot \mathbf{g}_e \cdot \mathbf{S} + S \cdot \mathbf{D} \cdot S + S \cdot \mathbf{A} \cdot \mathbf{I} - \mu_N \mathbf{B} \cdot \mathbf{g}_N \cdot \mathbf{I} + I \cdot \mathbf{Q} \cdot I. \quad (3)$$

All tensors have the trigonal form. For a magnetic field perpendicular to the trigonal axis the analysis predicts a central line flanked by satellites at the relative positions $-4Q$, $-2Q$, $+2Q$ and $+4Q$. The nuclear quadrupole interaction is determined from EPR as $Q/h \approx 4$ MHz. Numerical computer analysis of the full angular dependence confirms this value.

2.1.2. Second-order effects

Among the purely nuclear terms the nuclear Zeeman interaction $g_N \mu_N \mathbf{B} \cdot \mathbf{I}$ is present whenever a nucleus with non-zero spin is involved. For centres of lower than cubic symmetry and having $I \geq 1$ also the nuclear quadrupole interaction $I \cdot Q \cdot I$ affects the energy levels. Though these terms are not related to the quantum number m_S which is changed in the EPR experiment they still have an effect on eigenstates and energies. Their effect on energy differences as mea-

sured in the transitions is, however, usually small and appears only as a perturbation in second order. Careful determinations of line positions can nevertheless in favourable cases reveal these contributions. In silicon, with EPR linewidths often near 0.2 mT, these conditions are satisfied. In III-V compounds, on the other hand, lines tend to be broad and one may not expect to be able to observe the small nuclear shifts.

An example to illustrate these measurements comes from the sulphur pair in silicon. The centre has two sulphur atoms on nearest neighbour lattice sites resulting in trigonal symmetry. When singly ionized the centre has spin $S = 1/2$. By doping with the isotope ^{33}S (nuclear spin $I = 3/2$) the nuclear probe can contribute to the characterization of the centre. An EPR spectrum as measured for $\mathbf{B} \parallel [100]$ is shown in fig. 3. It will be analyzed with the Hamiltonian equation (3), with the zero-field splitting term omitted. The dominant central line corresponds to centres with only $I = 0$ sulphur nuclei; from its position follows $g_{e,xx} = 2.0007$. The next-highest intensity lines, four at equal distance, reveal the hyperfine interaction with ^{33}S ; the splitting gives $A_{xx}/h \approx 115$ MHz. Closer inspection shows that these lines are not at exactly equal distance, but that their precise separation is 4.10, 3.96 and 4.14 mT, consecutively. This closely follows a second-order calculation in which the line positions are obtained as

$$h\nu = g_{xx} \mu_B B + \frac{3}{2} A_{xx} + \frac{3}{4} A_{xx}^2 / g_{xx} \mu_B B + 30 Q_{xy}^2 / A_{xx}, \quad (4a)$$

$$h\nu = g_{xx} \mu_B B + \frac{1}{2} A_{xx} + \frac{7}{4} A_{xx}^2 / g_{xx} \mu_B B - 18 Q_{xy}^2 / A_{xx}, \quad (4b)$$

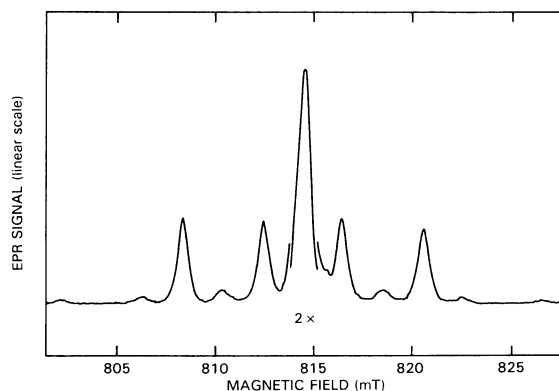


Fig. 3. EPR spectrum of the sulphur pair in silicon for magnetic field $\mathbf{B} \parallel [100]$, recorded in the microwave K-band. Due to the 25% enrichment in the isotope ^{33}S the spectrum is a superposition of $(\text{S}-\text{S})^+$ ($I = 0$), $(^{33}\text{S}-\text{S})^+$ ($I = 3/2$) and $(^{33}\text{S}-^{33}\text{S})^+$ ($I = 0, 1, 2, 3$) resonances. The $(^{33}\text{S}-^{33}\text{S})^+$ spectrum is a set of seven weaker lines with $m_I = 0, \pm 1, \pm 2$ and ± 3 with relative intensities of 4, 3, 2 and 1, respectively.

$$h\nu = g_{xx}\mu_B B - \frac{1}{2}A_{xx} + \frac{7}{4}A_{xx}^2/g_{xx}\mu_B B + 18Q_{xy}^2/A_{xx}, \quad (4c)$$

$$h\nu = g_{xx}\mu_B B - \frac{3}{2}A_{xx} + \frac{3}{4}A_{xx}^2/g_{xx}\mu_B B - 30Q_{xy}^2/A_{xx}. \quad (4d)$$

The result is $Q_{xy}/h = 2.46$ MHz. For this particular centre also a complete self-ENDOR project was carried out [10]. In this experiment the quadrupole parameter was determined with greater precision to be $Q_{xy}/h = 2.300$ MHz. The prior estimate for Q_{xy} from EPR greatly facilitated the difficult search for ENDOR.

A rather similar case is the Si: Ni_s⁻ centre [11]. Also this spin system has $S = 1/2$ and, when doped with the ⁶¹Ni isotope, $I = 3/2$. The bonding of the nickel atom in the silicon crystal leads to orthorhombic centre symmetry. The principal axes of the tensors are therefore along the $\langle 100 \rangle$ and two perpendicular $\langle 011 \rangle$ directions. An EPR spectrum with $B \parallel \langle 011 \rangle$ is shown in fig. 4. Again, the fourfold splitting confirms the presence of one nickel atom in the centre. Formulae similar to eqs. (4) can be derived to describe the spectrum quantitatively. The slight deviation from equidistant separation allows one to determine the quadrupole tensor. The principal values are calculated to be $Q_{[100]} \approx -2.1$ MHz, $Q_{[011]} \approx +4.5$ MHz and $Q_{[0\bar{1}1]} \approx -2.4$ MHz. In this case it was not (yet) possible to perform an ENDOR experiment due to the weakness of the signals. Therefore the careful fitting of precise EPR data provided the only way to obtain the nuclear terms.

2.2. Electron-nuclear double resonance

A more direct way to investigate the nuclear interactions is by ENDOR. As mentioned this method

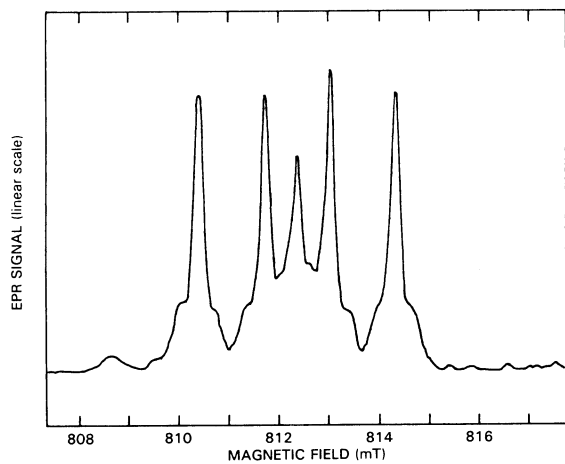


Fig. 4. EPR spectrum of substitutional nickel in silicon measured in K-band with magnetic field $B \parallel [011]$. Sample enriched to 88.1% in isotope ⁶¹Ni, nuclear spin $I = 3/2$.

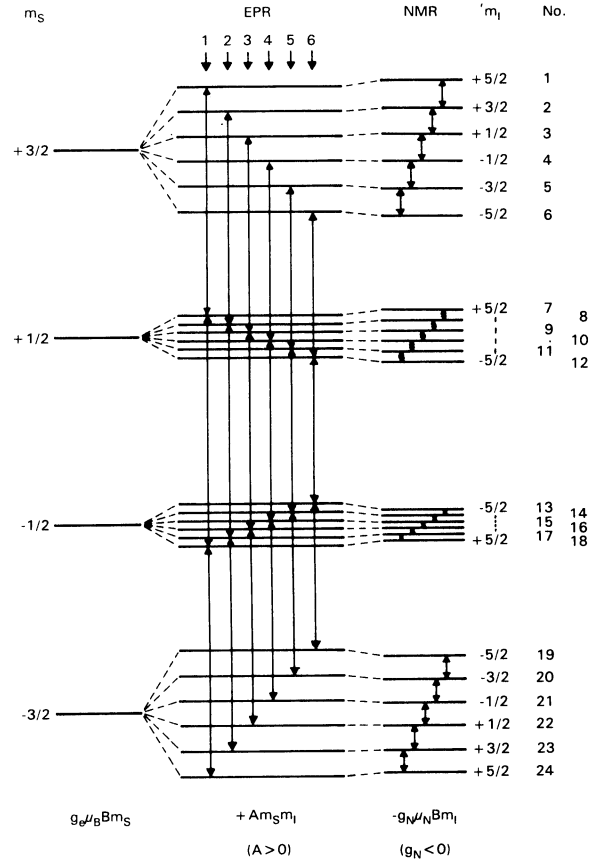


Fig. 5. Energy level diagram for spin system with electron spin $S = 3/2$ and nuclear spin $I = 5/2$, as applicable to Si: ⁴⁷Ti_i⁺, including electron Zeeman, hyperfine and nuclear Zeeman energies, but not to scale.

implies the simultaneous application of EPR and NMR. In addition to the EPR, transitions are induced between levels with different nuclear magnetization, via the nuclear Zeeman interaction term $g_N \mu_N I \cdot B \cos \omega t$. This operator will induce transitions following the selection rule $\Delta m_S = 0, \Delta m_I = \pm 1$. In ENDOR, the induction of the nuclear resonance is observed by an accompanying change of intensity of the underlying EPR. This transformation of radiofrequency quanta to microwave frequency quanta is the basis of the enhanced sensitivity of ENDOR over NMR. In order to be effective there must exist a coupling between the two resonances. A direct way to ensure this is by having a common energy level for the EPR and NMR transitions. This is illustrated in the diagram of fig. 5. For instance, the EPR transition $|m_S, m_I\rangle = |-1/2, -1/2\rangle \leftrightarrow |-3/2, -1/2\rangle$ and the NMR transition $|-3/2, -1/2\rangle \leftrightarrow |-3/2, +1/2\rangle$ both involve the level $|-3/2, -1/2\rangle$. The ENDOR related to this

level, i.e. level no. 21 in fig. 5, is shown in fig. 6. To low intensity double quantum transitions are also discernable.

The enhanced resolution of ENDOR allows the more accurate determination of the stronger nuclear interactions, such as nuclear Zeeman energy, hyperfine interaction and quadrupole energy, but also the observation of weaker interactions. The system of the titanium impurity in silicon provides an illustration [12]. Titanium occupies interstitial sites in silicon with no electrons used for bonding. In the positive charge state it has $3d^3$ electronic configuration, with, obeying Hund's rule, electron spin $S = 3/2$. Studies were made in samples in which the isotopes ^{47}Ti and ^{49}Ti were diffused to high enrichment. The isotopes have $I = 5/2$ and $I = 7/2$, respectively. Due to the high values of electron and nuclear spins, interactions of higher multipole character are possible. As the centre has cubic symmetry the Hamiltonian equation (1) is applicable. The frequencies of the transitions for this Hamiltonian will show no angular dependence. However, in the experiment an angular dependence was observed. When rotating the magnetic field in the (011) plane the frequencies show a variation proportional to

$$p(\theta) = 1 - 5 \sin^2\theta + \left(\frac{15}{4}\right) \sin^4\theta, \quad (5)$$

with θ the angle between \mathbf{B} and [100], for all transitions. Fig. 7 gives as a typical result the ENDOR related to level 16. These angular variations indicate the presence of interactions of higher order in the spins. To account for them the spin Hamiltonian has to be augmented by the fourth-order terms of form S^3I

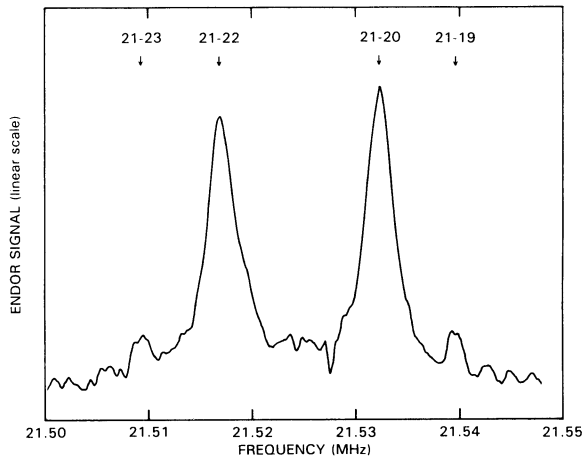


Fig. 6. ENDOR spectrum of Si: ^{47}Ti measured at temperature 4.2 K and magnetic field $\mathbf{B} \parallel [011]$ in the microwave K-band. The ENDOR is measured on EPR transition no. 3 and related to energy level no. 21 following the labeling of fig. 5.

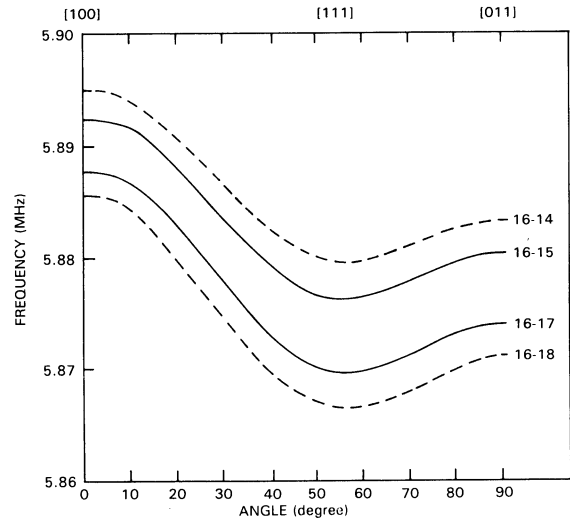


Fig. 7. Angular dependence of the ENDOR frequencies for rotation of the magnetic field in the (011) plane. The solid lines represent single quantum transitions; the dashed lines correspond to the weakly observable double quantum transitions. All transitions involve the level labeled no. 16 in fig. 5.

and S^2I^2 . Thus, to fit the experimental data following additional electron-nuclear terms were required:

$$H = +U\{S_x^3I_x + S_y^3I_y + S_z^3I_z - \left(\frac{1}{5}\right)[3S(S+1) - 1] \times (S_xI_x + S_yI_y + S_zI_z)\}, \quad (6)$$

$$H = +a[(S_xS_y + S_yS_x)(I_xI_y + I_yI_x) + \text{cyclic permutations}], \quad (7a)$$

$$H = +b\{[3S_x^2 - S(S+1)][3I_x^2 - I(I+1)] + \text{cyclic permutations}\}. \quad (7b)$$

With this Hamiltonian the coupling parameters for the nuclear interactions were found to an accuracy near 10 Hz.

In general the analysis of ENDOR spectra requires the measurement of angular dependence over a substantial range. This applies in particular to ligand ENDOR where, due to symmetry, atoms group together into shells and frequencies into patterns [13]. However, in the next example, the identification of an impurity is based on the observation of a single ENDOR line, without any detailed knowledge of its origin [14]. The ENDOR as shown in fig. 8 was measured on a silicon sample doped with ^{17}O , nuclear spin $I = 5/2$. The sample was subjected to heat treatment at 470°C creating the well-known thermal donors. When singly ionized these donors are $S = 1/2$ paramagnetic centres. This particular ENDOR experiment was carried out in a tunable variable-resonance-frequency cavity.

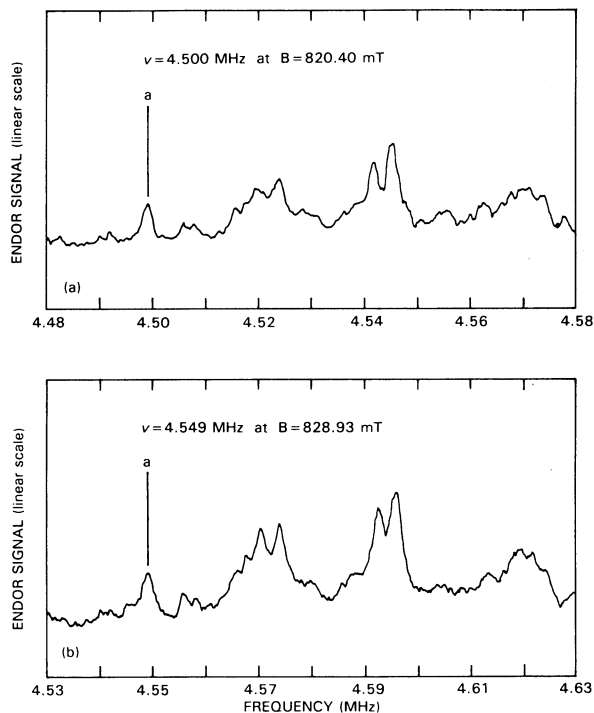


Fig. 8. ENDOR spectra observed for the Si-NL10 EPR spectrum related to thermal donors. The same transitions are recorded for two different values of the magnetic field. Data for line labeled a are discussed in text.

Upon comparing the results in figs. 8a and 8b, e.g. taking the resonance labeled a, one measures that, when changing the magnetic field by 8.53 mT, the ENDOR frequency changes by 49.2 kHz. To interpret the result a first-order solution of a Hamiltonian as eq. (3) is used. The energies are

$$E = +g_e\mu_B Bm_s + Dm_s^2 + Am_s m_l - g_N\mu_N Bm_l + Qm_l^2. \quad (8)$$

Recalling the ENDOR selection rules, i.e. $\Delta m_s = 0$, $\Delta m_l = \pm 1$, the ENDOR frequencies are found as

$$h\nu = +Am_s - g_N\mu_N B + 2Q(m_l - \frac{1}{2}). \quad (9)$$

In this approximation the frequency dependence on field is found as

$$d\nu/dB = -g_N\mu_N/h. \quad (10)$$

With the experimental result as quoted above one has $g_N\mu_N/h = 5.768$ MHz/T. From the nuclear tables one associates this result uniquely as due to oxygen. Therefore, without any cumbersome analysis but directly from a single measured line, the EPR spectrum Si-NL10 is concluded to be arising from a centre which contains the oxygen impurity.

3. Defect structure models

Interactions as probed in the magnetic resonance phenomenon are strongly related to the electric and magnetic fields in the centre. These same forces as generated by the nuclei and electrons composing the centre determine its structure. Therefore it is not surprising that the results of the magnetic resonance experiment, as represented by the spin Hamiltonian parameters, bear a direct relevance to defect structure. Two examples of interpretation will be discussed in the following.

For the centre GaP:Mn the results of EPR and ENDOR are summarized as follows: electron spin $S = 5/2$, nuclear spin $I = 5/2$, one nucleus 100% abundant, $g_e = 2.0011$, $g_N\mu_N/h = (10.3 \pm 0.2)$ MHz/T, $A/h = (\pm)266.42$ MHz, zero-field term $D = 0$, cubic field term a not measurable, quadrupole interaction $Q = 0$ [5]. The sixfold splitting of the EPR spectrum, six lines of equal intensity at equal distance (see fig. 1), indicates the presence of a single nucleus with spin $I = 5/2$. Other isotopes with different spin would have given resonances at other positions. For instance, zero spin isotopes would have given a line at the centre position. This is not observed. It limits the candidates to Al, Mn, and the more exotic ones I, Pr and Re. Both in EPR and ENDOR the nuclear g -value was determined. Whereas the limited accuracy of EPR could not discriminate between Al and Mn, the ENDOR result unambiguously selects Mn. The electron spin of the centre is measured to be $5/2$. Since the symmetry of the centre is cubic there might be an orbital contribution to this spin, e.g. in a triplet ground state. However, the measured electronic g -value, $g_e = 2.0011$, is close to the free electron value, indicating the absence of orbital momentum. The groundstate is therefore regarded as a ${}^6S_{5/2}$ state and its spin derives from five parallel electron spins. A half filled d-shell following Hund's rules has the required $L = 0$, $S = 5/2$. For the manganese then the most likely electronic configuration is $[\text{Ar}]3d^5$, corresponding to Mn^{2+} . An alternative is the neutral configuration $[\text{Ar}]3d^5 4s^2$. To distinguish between these configurations the hyperfine interaction can be considered. An isotropic interaction with constant $A/h = 266.42$ MHz was measured. Being isotropic the interaction arises from contact spin density which can be given by electrons in 1s, 2s, 3s and 4s states. The filled s shells are polarized by the spin of the d electrons. The polarizations are given in the literature [15] as $A/h = 304$ MHz for 1s–3s and $A/h = 48$ MHz for 1s–4s. Therefore the measured value is inconsistent with occupation of the 4s orbitals. Compared to the value for 1s–3s core polarization the measured value represents a slight reduction. This could be accounted for by covalent delocalization of the d electrons or by having some density in bonding

orbitals involving 4s electrons. This issue is related to the site of the manganese impurity in the crystal. All data indicate the highest possible symmetry of the centre. All measured interactions are isotropic and interactions occurring in lower symmetry, such as zero field splitting D and quadrupole interaction, are absent. The manganese ion will occupy a site of cubic, pointgroup T_d , symmetry. Four such sites are present in the GaP crystal: the two substitutional sites on the Ga and P sublattices, respectively, and two interstitial sites. On the substitutional sites substantial bonding between impurity and nearest neighbour atoms is expected. The bonding orbitals will accommodate some electron density in 4s orbitals leading to reduction of the hyperfine interaction. An empirical relation has been established linking the hyperfine constant to the degree of covalency of the bonds [16]. This curve, based on a large number of Mn^{2+} observations, is given in fig. 9. For the Mn ion on a substitutional site, either on the gallium or the phosphorus sublattice, the hyperfine interaction would be represented by the

points labeled GaP_{Ga} and GaP_P , respectively, in fig. 9. Since these points fall far outside the curve accommodation of Mn as a substitutional impurity is concluded to be highly unlikely. Besides, substitutional Mn on the Ga site has been observed before [17] and its data nicely fit the curve. Manganese as observed in the present EPR spectrum thus corresponds to an interstitial impurity. Similar arguments as presented above lead to the preference of the interstitial site which is surrounded by four Ga atoms as nearest neighbours. The reduction by about 12% of the hyperfine interaction of the interstitial manganese compared to the free ion can be understood by some covalent delocalization of the d electrons. For the ion on the interstitial site this effect is therefore small, which is consistent with the remarkably small linewidth of the resonances. In this sequence of arguments the centre has been identified as a single manganese impurity, occupying a high-symmetry interstitial site, and, while being observed as Mn^{2+} , as a double donor. Magnetic resonance measurements thus provided the first detection of a transi-

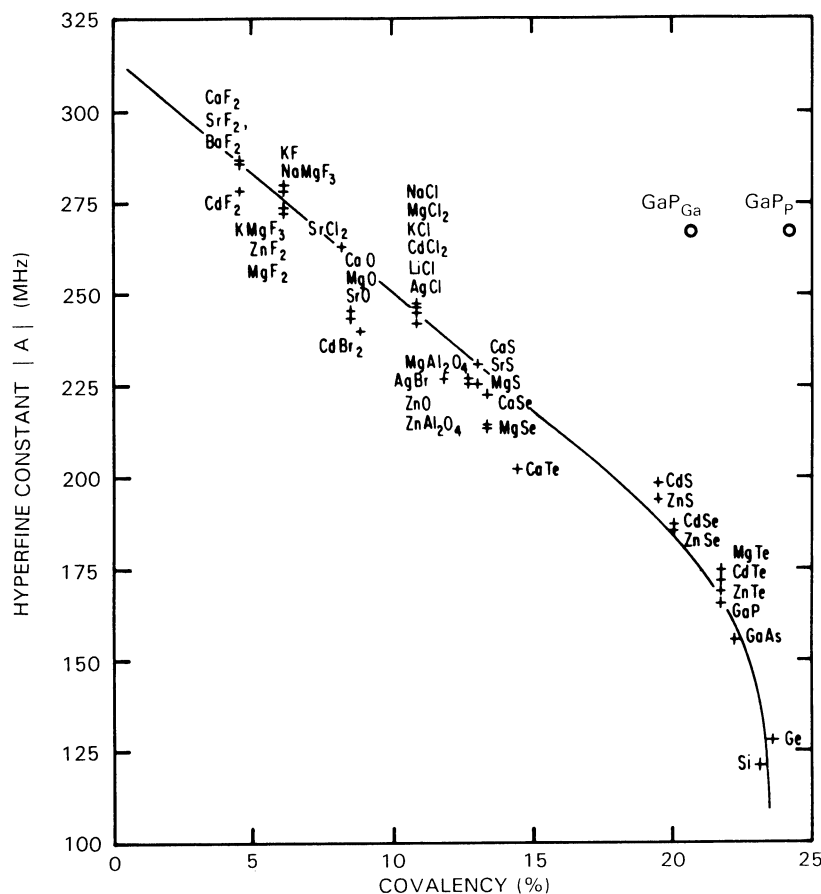


Fig. 9. Empirical relation between the absolute value of the hyperfine constant A and covalency of the bonds between Mn and its nearest neighbours for substitutional Mn in various compounds. Points GaP_P and GaP_{Ga} are discussed in the text.

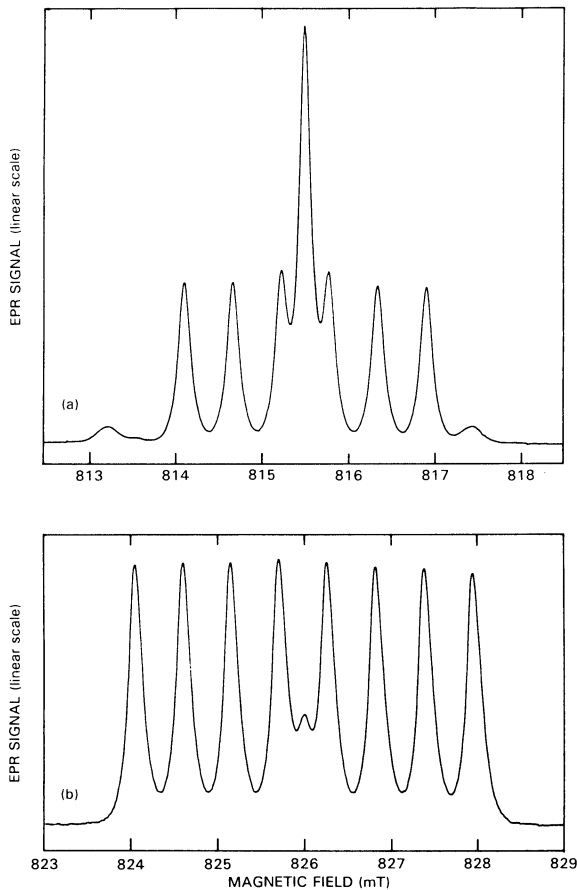


Fig. 10. EPR spectrum for interstitial titanium in silicon measured in K-band; (a) enriched to 68.5% in isotope ^{47}Ti , $I = 5/2$, (b) enriched to 96.25% in isotope ^{47}Ti , $I = 7/2$. The central lines correspond to the $I = 0$ isotopes.

tion metal impurity on an interstitial site in a compound semiconductor, as well as further characterization of its electronic structure.

In the second example, interstitial titanium in silicon, magnetic resonance is up to date also the only technique available to identify and monitor the centre. Its identification is based on EPR measurements, reproduced in fig. 10 [12, 18]. The spectrum is isotropic, indicating a site of cubic symmetry. In the silicon crystal two such sites, one substitutional and one interstitial, are available. The EPR line splits under application of uniaxial stress revealing spin $S = 3/2$ for the centre. This matches without any difficulty a ${}^4\text{A}_2$ (t_2^3) ground state of Ti^+ on an interstitial site. For a substitutional position no easy explanation would be possible. As directly visible in the EPR spectrum, both isotopes have an almost equal hyperfine interaction. Analysis of the ENDOR data gives $A/h = 15.64505$ MHz for ^{47}Ti and $A/h = 15.65070$ MHz for ^{49}Ti . This, of course, is directly related to the known nearly equal

nuclear g values of the isotopes. As measured by ENDOR the values are $g_{\text{N}} = -0.315139$ for ^{47}Ti and $g_{\text{N}} = -0.315219$ for ^{49}Ti . The hyperfine interaction is isotropic and is related to spin in s orbitals having contact interaction with the nucleus. The measured values are related to this spin density $\delta\rho$ via

$$A = \frac{1}{2S} \frac{2}{3} \mu_0 g_{\text{e}} \mu_{\text{B}} g_{\text{N}} \mu_{\text{N}} \delta\rho, \quad (11)$$

and one finds $\delta\rho = 1.26 \times 10^{30} \text{ m}^{-3}$. Probably, $1s$ – $3s$ core polarization gives the main contribution to the spin density. The published calculated value amounts to $5.2 \times 10^{30} \text{ m}^{-3}$ for a $3d^3$ configuration [15]. A substantial reduction is therefore found. It can be explained by assuming covalently delocalized orbitals with a localization on titanium $3d$ orbitals of 24%. Indeed, the ligand ENDOR measurements of the centre have indicated a minimum delocalization into the crystal of 40% [19]. The availability of two nuclear magnetic isotopes with high spin allowed the investigation of non-common electron–nuclear interactions. For instance, precise calculation reveals that the spin density does not appear to be exactly equal on the two nuclei when using eq. (11). Instead, one would obtain $\delta\rho = 1.25863 \times 10^{30} \text{ m}^{-3}$ for ^{47}Ti and $\delta\rho = 1.25877 \times 10^{30} \text{ m}^{-3}$ for ^{49}Ti . A small, but measurable, hyperfine anomaly exists, which is a manifestation of the different distribution of nuclear magnetic dipole moment in these nuclei. In section 2.2 of this paper it was shown that the analysis of ENDOR data for titanium required higher-order electron–nuclear interaction terms of form S^3I and S^2I^2 . Attempts have been made to interpret these results in crystal field theory. In particular for the S^3I term no satisfactory calculation has been presented up to now. The term S^2I^2 can represent an interaction between electronic and nuclear quadrupole moments. For this interaction the expressions

$$a = - \left(\frac{3n}{4} \right) \frac{e^2 Q \langle r^{-3} \rangle}{I(2I-1)} \quad (12a)$$

$$b = - \left(\frac{m}{6} \right) \frac{e^2 Q \langle r^{-3} \rangle}{I(2I-1)} \quad (12b)$$

were derived [20]. If this is the measured interaction, one expects

$$\begin{aligned} a(^{49}\text{Ti})/a(^{47}\text{Ti}) &= b(^{49}\text{Ti})/b(^{47}\text{Ti}) \\ &= 10Q(^{49}\text{Ti})/21Q(^{47}\text{Ti}), \end{aligned} \quad (13)$$

with Q the nuclear electric quadrupole moments. Using the experimental data one finds for these ratios 0.38 ± 0.02 and 0.42 ± 0.11 for a and b , respectively. For the quadrupole moments one finds, using literature values, the ratio 0.39 ± 0.02 . It can thus be concluded that the interaction is due to nuclear–electronic

quadrupole interactions. The electric field gradient in the cubic titanium ion arises from the admixture of higher states into its ground state.

References

- [1] F. Bloch, Phys. Rev. 70 (1946) 460.
- [2] F. Bloch, W.W. Hansen and M. Packard, Phys. Rev. 70 (1946) 474.
- [3] E. Zavoisky, J. Phys. (Acad. Sci. USSR) 9 (1945) 245, 211.
- [4] G. Feher, Phys. Rev. 114 (1959) 1219.
- [5] S.J.C.H.M. van Gisbergen, M. Godlewski, T. Gregorkiewicz and C.A.J. Ammerlaan, Phys. Rev. B44 (1991) 3012.
- [6] E. Friedman and W. Low, Phys. Rev. 120 (1960) 408.
- [7] V.J. Folen, Phys. Rev. 125 (1962) 1581.
- [8] B.C. Cavenett, Proc. Phys. Soc. 84 (1964) 1.
- [9] H.E. Altink, T. Gregorkiewicz and C.A.J. Ammerlaan, Solid State Commun. 75 (1990) 115.
- [10] A.B. van Oosten and C.A.J. Ammerlaan, Phys. Rev. B38 (1988) 13291.
- [11] L.S. Vlasenko, N.T. Son, A.B. van Oosten, C.A.J. Ammerlaan, A.A. Lebedev, E.S. Tapygov and V.A. Khramtsov, Solid State Commun. 73 (1990) 393.
- [12] D.A. van Wezep and C.A.J. Ammerlaan, Phys. Rev. B37 (1988) 7268.
- [13] M. Sprenger, S.H. Muller, E.G. Sieverts and C.A.J. Ammerlaan, Phys. Rev. B35 (1987) 1566.
- [14] T. Gregorkiewicz, D.A. van Wezep, H.H.P.Th. Bekman and C.A.J. Ammerlaan, Phys. Rev. Lett. 59 (1987) 1702.
- [15] R.E. Watson and A.J. Freeman, in: Hyperfine Interactions, eds. A.J. Freeman and R.B. Frankel (Academic Press, New York, 1967) p. 53.
- [16] E. Šimánek and K.A. Müller, J. Phys. Chem. Solids 31 (1970) 1027.
- [17] P. van Engelen and S.G. Sie, Solid State Commun. 30 (1979) 515.
- [18] D.A. van Wezep and C.A.J. Ammerlaan, J. Electron. Mater. 14A (1985) 863.
- [19] D.A. van Wezep, R. van Kemp, E.G. Sieverts and C.A.J. Ammerlaan, Phys. Rev. B32 (1985) 7129.
- [20] B. Bleaney, in: Hyperfine Interactions, eds. A.J. Freeman and R.B. Frankel (Academic Press, New York, 1967) p. 1.